ELSEVIER

Thermochimica Acta 388 (2002) 299–312

thermochimica acta

www.elsevier.com/locate/tca

# A description of chemical and diffusion control in isothermal kinetics of cure kinetics

J.E.K. Schawe

*Mettler-Toledo GmbH, Sonnenbergstrasse 74, CH-8603 Schwerzenbach, Switzerland*

Received 16 August 2001; received in revised form 3 October 2001; accepted 4 October 2001

**Abstract**

During isothermal polymerization reaction, a thermosetting resin vitrifies if the reaction temperature is lower than the maximum glass transition temperature of the fully reacted material. Due to the vitrification process, the kinetics become diffusion-controlled. The kinetics of such reactions can be described using a diffusion control function. The actual reaction rate can be expressed as a product of the reaction rate of the chemically controlled reaction and the diffusion function.

It is shown that the chemically controlled kinetics can be evaluated using isoconversional methods (model-free kinetics) from DSC heating experiments at sufficiently high heating rates. For the diffusion control function, a new phenomenological expression is introduced which is independent from the reaction temperature and requires only one parameter. This parameter can be interpreted as the width of the glass transition.

The presented approach can be used to predict the kinetics of complex reactions including the change from chemically controlled to diffusion-controlled kinetics, on the basis of a small number of experiments. 

*Keywords:* Kinetics; Vitrification; Diffusion control; Thermosets; Cure; Polymerization

## 1. Introduction

The kinetics of competing chemical reactions are usually described by:

$$\frac{d\alpha}{dt} = \sum_{p=1}^{q} f_p(\alpha) k_p(T) \tag{1}$$

in the simplest case, the reaction is represented by only one function $f$ and one rate constant $k$:

$$\frac{d\alpha}{dt} = f(\alpha) k(T) \tag{2}$$

where, $\alpha$ is the extent of reaction (conversion), $f(\alpha)$ the conversion function describing the reaction model, and $k(T)$ corresponds to the Arrhenius law,

$$k(T) = k_0 \exp\left(-\frac{E_a}{RT}\right) \tag{3}$$

where, $E_a$ denotes the activation energy of the reaction and $R$ the gas constant [1]. By DSC measurements the mechanism of the reaction cannot be investigated in detail. The problem, therefore, consists in finding a kinetic model, which describes the investigated reaction properly. Collections of related models are given in the literature (e.g. [2]).

In the case of epoxy curing, the chemically controlled reaction can be modeled by a semi-empirical autocatalytic rate equation with two conversion

*E-mail address:* juergen.schawe@mt.com (J.E.K. Schawe).

0040-6031/02/$ – see front matter 
PII: S0040-6031(02)00041-2

functions $f_1 = (1-\alpha)^n$ and $f_2 = \alpha^m f_1$ [3,4]:

$$\frac{d\alpha}{dt} = (k_1 + k_2\alpha^m)(1-\alpha)^n \quad (4)$$

The glass transition temperature of a curing system increases with the increasing conversion during reaction [5]. If a thermosetting systems react below the maximum glass transition temperature, the material transforms from a liquid state into a glassy state. This vitrification process occurs when the actual glass transition temperature $T_g$ reaches the curing temperature. During vitrification the reaction rate slows down because the reaction becomes diffusion-controlled [6–8]. Since this transition from a chemically to a diffusion-controlled reaction scheme occurs gradually, one has to correct a conventional reaction model by a conversion-dependent diffusion contribution. For thermosetting systems, it has been suggested to modify Eq. (2) or (4) by a ''diffusion control function'' $f_d(\alpha)$ which takes into account the reduced molecular mobility due to the network formation process [9]:

$$\frac{d\alpha}{dt} = \left[\frac{d\alpha}{dt}\right]_{chem} f_d(\alpha) \quad (5)$$

where, $[d\alpha/dt]_{chem}$ describes the chemically controlled kinetics related to Eqs. (1)–(4). If the reaction is chemically controlled, $f_d$ is unity. In the case of full diffusion control, the reaction is practically interrupted and the diffusion control function is zero. A further explanation of the meaning of $f_d$ is given in the Appendix A in context with conventional kinetic approaches. Fournier et al. [9] proposed an empirical function

$$f_d(\alpha) = 2\left(1 + \exp\left(\frac{\alpha - \alpha_f}{b}\right)\right)^{-1} - 1 \quad (6)$$

where, $\alpha_f$ is the final conversion and $b$ an empirical parameter. For the isothermal cure of the thermosetting system diglycidylether of bisphenol A (DGEBA) and diaminodiphenyl methane (DDM) Jenninger et al. [10] have applied a combination of Eqs. (4)–(6) for kinetic evaluation by curve fitting. Agreement between the fit and the measure curve decreases with the increasing temperature. It was shown that the model fits the experimental data at a reaction temperature of 80 °C reasonably well. However, at a reaction temperature of 120 °C, there is less agreement between the measured data and the fit curve. This result can be an indication for insufficiency of the used model. As discussed at Brown and Galswey [11], to distinguish amongst the different possible models for the kinetics is not an easy task.

A completely different approach is offered by model-free kinetics. In this approach, it is assumed that complex reactions can be described by a conversion-dependent activation energy. The activation energy can no longer be understood in the sense of Arrhenius but more in terms of an apparent activation energy, in which the diffusion or nucleation processes are included as well. Formally, model-free kinetic analysis is based on an isoconversional principle, according to which the reaction rate, $d\alpha/dt$, at constant extent of conversion, $\alpha$, is a function of the temperature only. Several authors have developed different isoconversional methods [12–14]. Knowledge of conversion-dependent activation energy is sufficient to reliably predict the kinetics of a reaction in a wide temperature range [15].

In the literature, the model-free kinetic approach is used for analyses of the kinetics of thermosetting systems. Usually the apparent activation energy decreases due to vitrification process [16–18].

The activation energy curve $E_a(\alpha)$ becomes dependent on experimental conditions when the reaction changes from chemically to diffusion controlled because the vitrification process strongly depends on temperature and heating rate. In such a case, a general prediction of the kinetic behavior in a wide temperature range using model-free kinetics is restricted.

In the present paper, we describe the isothermal reaction kinetics of thermosets in a large temperature range by combining the model-free kinetics with a phenomenological vitrification function. To do this, a new model function for $f_d(\alpha)$ is suggested which only has one parameter that can be determined by independent measurements. As in a recent publication [19], model-free kinetics are used for the evaluation of the chemically controlled reaction rate in Eq. (5).

## 2. Experimental

### 2.1. Sample

Commercial DGEBA (Shell Chemical, Epikote 828) and DDM (Aldrich) were used as a thermosetting system. The substances were poured together in the

stoichiometric amounts of 2 mol DGEBA and 1 mol DDM and heated up to 120 °C for 20 s. During this time, the sample was stirred to get a homogeneous mixture. The mixture was then rapidly cooled to room temperature and approximately 3 mg samples were prepared in aluminum crucibles. The samples were stored at −30 °C.

### 2.2. Instrumentation

The measurements were performed on a METTLER TOLEDO DSC 822$^e$ with intra-cooler using the ''Model-free kinetics'' software option for kinetic evaluation. The instrument was temperature calibrated with water, indium and tin. Indium was used for the heat flow calibration. The furnace atmosphere was defined by 50 ml/min nitrogen.

## 3. Results

### 3.1. Temperature scanning measurements (ramp curing)

The ''classical'' experiment is a linear heating run of the initial reaction mixture from a temperature below glass transition to the end of the curing reaction. The heating rate varied between one and 10 K/min. The set of measured curves normalized in heat capacity units is shown in Fig. 1.

Whereas, the glass transition (around −15 °C) is nearly independent of the heating rate (temperature shift: ≈4 K per decade heating rate), the peak temperature of the cure reaction shows a large shift to higher temperatures by increasing heating rate. This shift is in the order of 60 K per decade heating rate. For the curve measured with 1 K/min, a shoulder appears in the temperature range between 130 and 160 °C. This is an indication for a change in kinetics during cure. From the curve measured with 10 K/min the specific heat of reaction was determined to be $\Delta h_r = 407$ J/g.

### 3.2. Isothermal measurements

From isothermal DSC measurements at curing temperatures between 40 and 170 °C, the conversion curves are calculated. The main problem of isothermal measurements is the missing part of reaction during heating of the sample to curing temperature. To reduce such uncertainties the sample was rapidly cooled down to −20 °C after the isothermal measurement

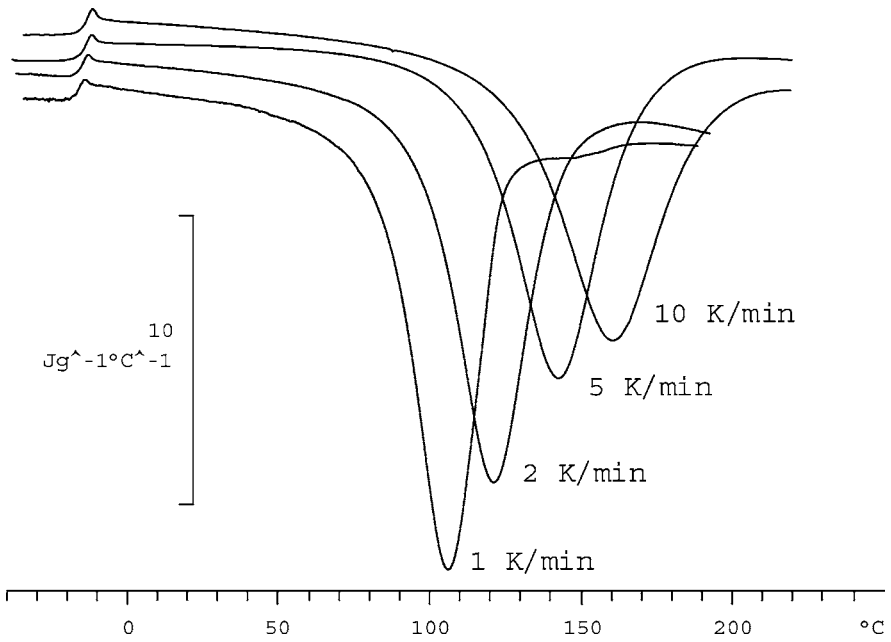


Fig. 1. DSC curves measured with different heating rates, normalized in heat capacity units.

and heated up again with 10 K/min. At this post-curing measurement, a reaction peak occurs due to the remaining unreacted part. The related peak area $\Delta H_p$ is determined. Conversion as a function of the reaction time during isothermal reaction can then be calculated by the equation

$$\alpha(t_{react}) = 1 + \frac{1}{m\Delta h_r} \times \left( \int_0^{t_{react}} \Phi(t')\,dt' - \int_0^{t_{end}} \Phi(t')\,dt' - \Delta H_p \right) \quad (7)$$

where, $\Phi$ is the heat flow measured in the isothermal experiment and $t_{end}$ is the maximum reaction time. Selected curves of conversion versus the reaction time are shown in Fig. 2.

### 3.3. Post-curing measurements

The reaction kinetics and the glass transition can be simultaneously investigated in the so-called post-curing experiment after the isothermal cure for different reaction times $t_{react}$. After the isothermal cure the sample is rapidly cooled below the glass transition temperature. Then the sample is heated up with a given heating rate (e.g. 10 K/min). In the next step, a new fresh sample is used for the same procedure with a different reaction time [20]. As a result, we obtain a set of DSC curves for one reaction temperature. For the reaction temperature of 100 °C, the set of post-curing curves is shown in Fig. 3.

With increasing reaction time, the glass transition increases. For long curing, the glass transition temperature is above the reaction temperature. Above the glass transition the curing reaction starts again. From this exothermal reaction peak the specific enthalpy of post-curing $\Delta h_p$ is determined.

At sufficiently long isothermal cure, the reaction in a post-curing experiment starts immediately after the glass transition. The residual conversion is relatively low and the glass transition shows a large enthalpy relaxation peak. For these reasons the post-curing curve must be evaluated carefully. The applied evaluation procedure for $\Delta h_p$ and the glass transition temperature $T_g$ is shown in Fig. 4. For the enthalpy determination, the baseline of the reaction peak must be found. Richardson has suggested to use the curve of the fully cured material for the construction of the baseline [21]. To simplify the following evaluation steps we extrapolate the normalized heat flow curve above the glass transition to lower

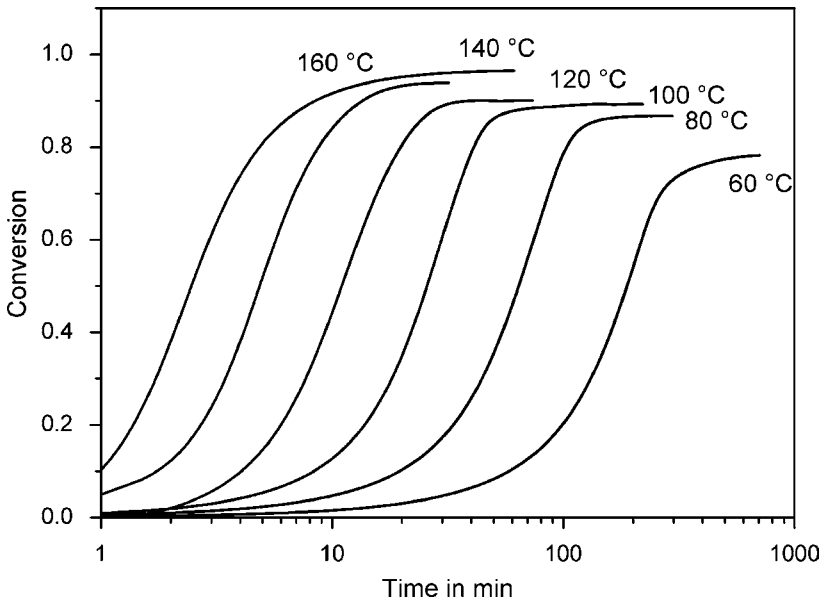


Fig. 2. Conversion as a function of the reaction time measured in isothermal experiments at different reaction temperatures.

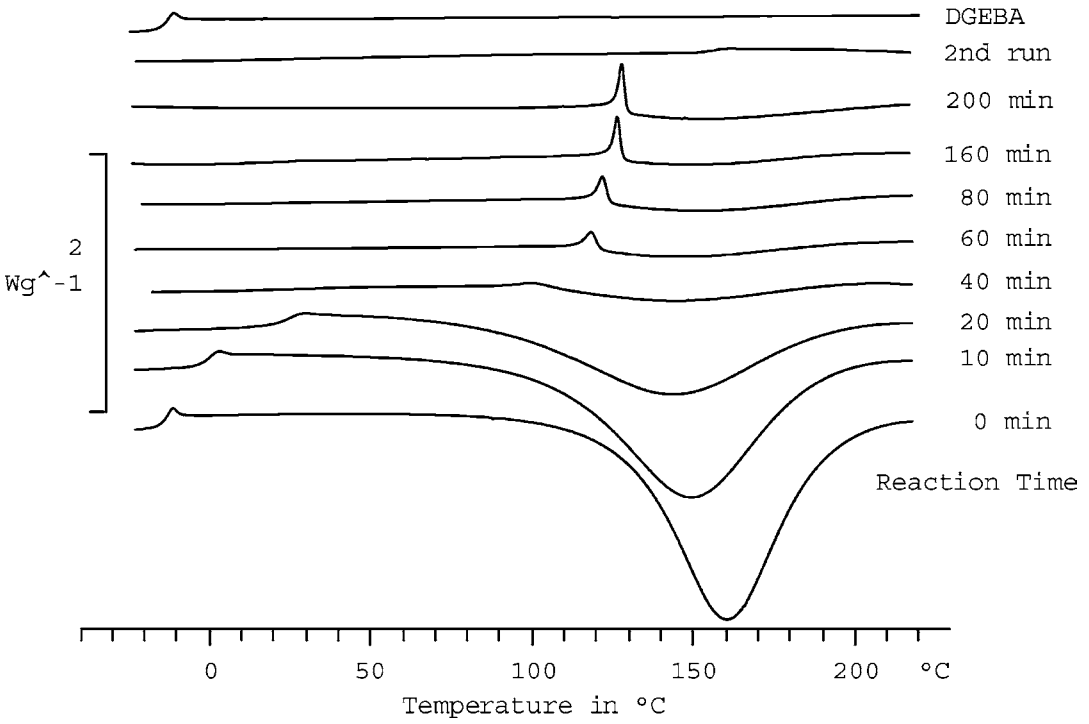


Fig. 3. Specific heat flow vs. the sample temperature measured by a post-curing experiment (exothermal heat flow is downwards). Before this measurement, the resin was cured at 100 °C for the given time. The heating rate was 10 K/min. For comparison the curves of the fully cured material (second run) and the pure DGEBA without curing agent is also plotted.

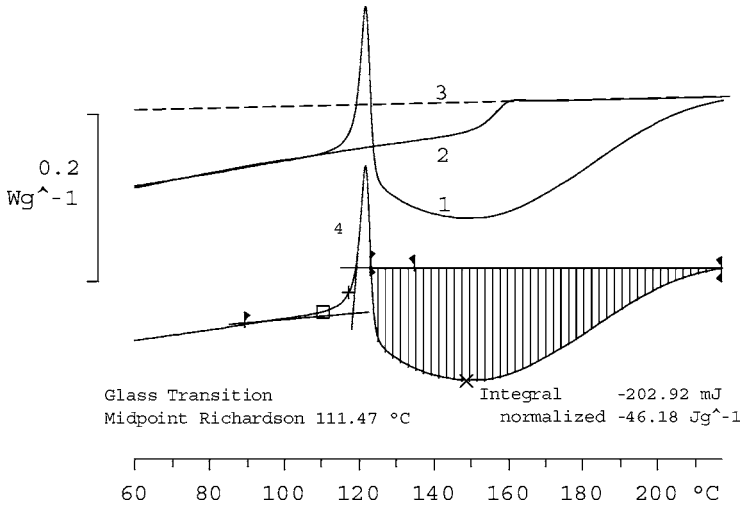


Fig. 4. Example of the evaluation of post-curing curves (exothermal heat flow direction is downwards). The sample was cured for 80 min at 100 °C. (1: post-curing curve, 2: curve of the fully cured material, 3: extrapolated line from the liquid region of the fully cured material, 4: difference of curves 1 and 3 to get a horizontal baseline.

temperatures (line 3). This line is subtracted from the measured curve 1 to get a horizontal baseline in the resulting curve 4. From this curve the specific enthalpy of the post-curing $\Delta h_p$ is calculated. The same horizontal line is used for the evaluation of the glass transition temperature. $T_g$ was determined as a ''fictive temperature'' using the algorithm described by Richardson [21]. This procedure for determining $T_g$ is applied to minimize the influence of the enthalpy relaxation on the result. The fictive temperature is a characteristic temperature of the glass transition. At this temperature, an equilibrated liquid has the same structure (entropy) as the actual glass.

The conversion after the isothermal cure for $t_{react}$ at $T_{react}$ is:

$$\alpha(t_{react}) = \frac{\Delta h_r - \Delta h_p}{\Delta h_r} \tag{8}$$

The glass transition temperature and the conversion as a function of the curing time determined from Fig. 3 is shown in Fig. 5.

The vitrification time $t_v$ is defined as the reaction time at which the glass temperature becomes equal to the reaction temperature. It is determined to be 48 min. During vitrification the material transforms in the glassy state. Consequently, the molecular mobility and the molecular diffusion processes show a chemical induced freezing-in and the chemical reaction rate slows down. The final conversion remains practically constant below unity. The glass transition temperature for large reaction times is approximately 10 K above the reaction temperature.

### *3.4. The glass transition temperature as a function of conversion*

The data of Fig. 5 are used for the construction of the glass transition temperature versus conversion diagram (Fig. 6). The glass transition temperature of the fully cured material ($\alpha = 1$) was determined by a second run with 10 K/min.

For the description of this functional relationship, different equations are suggested [20,22,23]. The DiBenedetto equation (Eq. (9)) is frequently used

$$T_g(\alpha(t_{react})) = \frac{\lambda\alpha(t_{react})(T_{g1} - T_{g0})}{1 - (1 - \lambda)\alpha(t_{react})} + T_{g0} \tag{9}$$

where, $\lambda$ is a fit parameter, $T_{g0}$ and $T_{g1}$ are the glass transition temperatures of the uncured and the fully reacted material, respectively. By curve fitting of the data in Fig. 6, we get $\lambda = 0.31$ and $T_{g1} = 169.3\ ^\circ C$. The glass transition temperature of the initial mixture $T_{g0}$ was taken to be $-18.3\ ^\circ C$. This is the measured value of the related curve in Fig. 3.

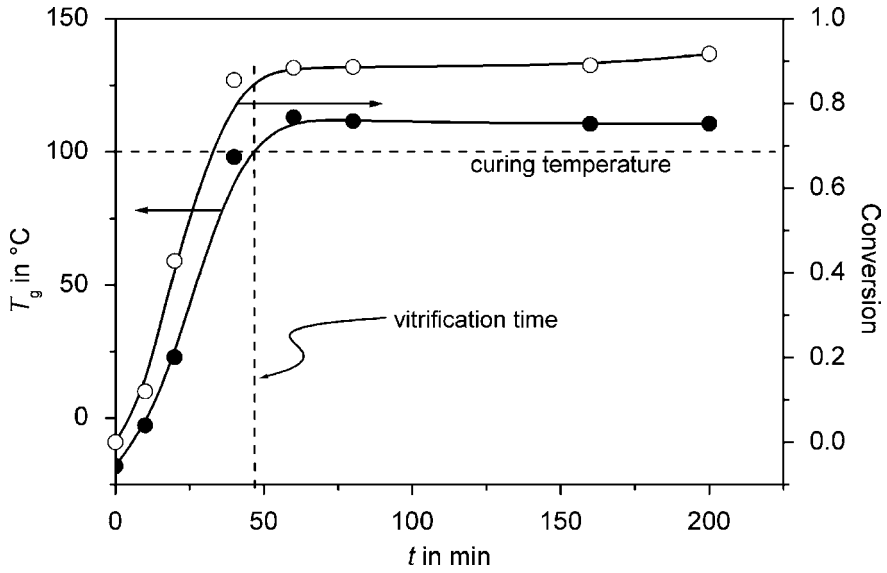


Fig. 5. Glass transition temperature and conversion as a function of the reaction time. The data are evaluated from the curves in Fig. 3.

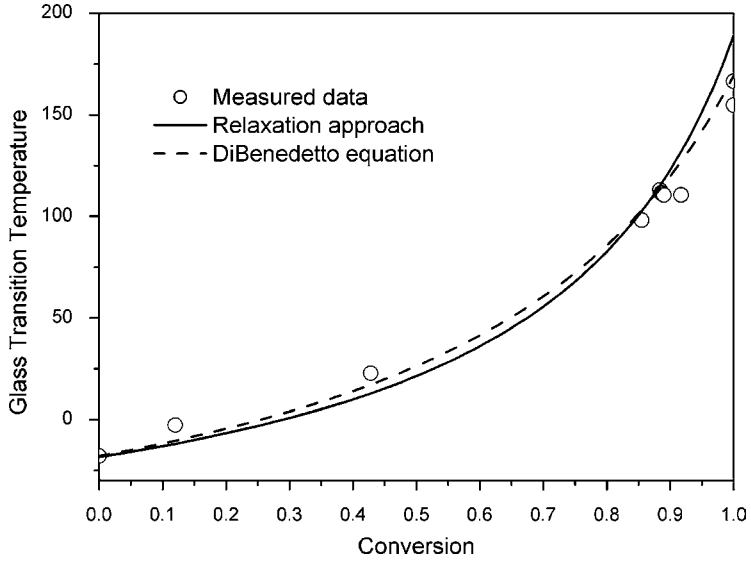


Fig. 6. Glass transition temperature vs. conversion. Data based on Figs. 3 and 5. The lines represent different fit curves using the DiBenedetto equation (Eq. (8)) and the equation derived from the relaxation approach (Eq. (9)), respectively.

Another equation follows from the relaxation approach [23]:

$$T_g(\alpha) = T_{g1} + C_2 + \frac{DT_{g1}}{1/(x_0 - 1) - DT_{g1}/C_2 - 1/x_0 - \alpha} \tag{10a}$$

where,

$$x_0 = \frac{1}{2} + \sqrt{\frac{1}{4} + \frac{C_2(T_{g1} - T_{g0} + C_2)}{DT_{g1}(T_{g1} - T_{g0})}} \tag{10b}$$

$D$ is the fragility parameter and $C_2$ the difference between the glass transition temperature (determined by DSC with 10 K/min) and the Vogel-temperature.

With $T_{g0} = -18.3$ °C the parameters are $D = 2.178$, $C_2 = 29.35$ K (this gives a value of $x_0 = 1.032$ from Eq. (10b)) and $T_{g1} = 189.1$ °C. The determined value of $T_{g1}$ is larger than the measured value in a scanning experiment at 10 K/min (154.8 °C). The difference is an indication of the experimental uncertainty of $T_{g1}$. For low heating rates and isothermal measurements at high temperatures, larger final glass transition temperatures are determined for a wide class of thermosetting systems [24]. In our system, for investigation, we observed the following "final" glass transition temperatures $T_{g1}$ after different thermal history.

A 154.8 °C (after heating with 10 K/min), 166.5 °C (after isothermal cure at 100 °C for 300 min), 169.3 °C (after isothermal cure at 170 °C for 100 min) and 189.1 °C (extrapolated from Eq. (10)). For the measure of $T_{g1}$ after the thermal treatment, the sample was heated to 220 °C with 10 K/min and then rapidly cooled to room temperature. The $T_g$ measurements were carried out on the second heating curve with 10 K/min.

## 4. Discussion

### 4.1. Kinetics of the chemically controlled reaction

The conversion as a function of temperature can be calculated directly from the measured curves of Fig. 1:

$$\alpha(T) = \frac{\int_{T_0}^{T} (\Phi(T') - \Phi_{BL}(T'))\,dT'}{m\beta\Delta h_r} \tag{11}$$

where, $\Phi$ is the measure heat flow curve, $\Phi_{BL}$ represents the baseline, $\beta$ the heating rate, $m$ the sample mass and $\Delta h_r$ the specific enthalpy of reaction. $T_0$ is a reference temperature before the reaction starts. Such conversion curves are shown in Fig. 7.

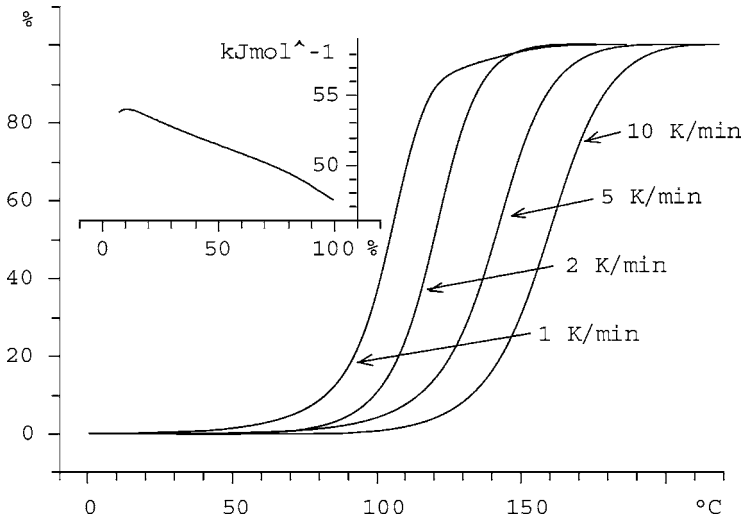


Fig. 7. Conversion in percent as a function of the sample temperature at different heating rates. Curves are calculated from the measured curves of Fig. 1. In the inset, apparent activation energy $E_a$ vs. conversion is shown. $E_a$ is determined using the isoconversional method (model-free kinetics).

The reaction becomes diffusion-controlled as soon as the glass transition temperature of the curing system exceeds the actual reaction temperature. In the case of the ramp curing experiments in Fig. 1, the change of the glass transition temperature during reaction can be calculated if the function $T_g(\alpha)$ is known. The calculated glass transition temperature and the sample temperature during ramp curing is plotted in Fig. 8. For the calculation of $T_g$ the actual maximum value $T_{g1}$ (measured in the second run) is used. In Fig. 8 it is clearly shown that at a heating rate of 1 K/min the glass transition temperature exceeds the sample temperature in the temperature range between 120 and 150 °C. In this range the reaction kinetics are influenced by diffusion control. Using 2 K/min there is practically no contribution of diffusion control.

The model-free kinetics tool in the Mettler-Toledo STAR$^e$-software on the basis of the approach of Vyazovkin [25] delivers the apparent conversion-dependent activation energy. For the calculation, DSC curves measured at scanning rates between 20 and 2 K/min are used. The resulting activation energy curve $E_a(\alpha)$ is shown in the inset of Fig. 7. $E_a$ decreases slightly with the increasing conversion. The average value is approximately 52 kJ/mol. This is an indication for a constant reaction mechanism in the range $0.2 \leq \alpha \leq 1$ for the used experimental conditions.

On the basis of the evaluated curve $E_a(\alpha)$, the isothermal conversion curves can be simulated [16]. They represent the chemically controlled reaction:

$$\alpha_{chem}(t) = \int_{t_0}^{t} \left[\frac{d\alpha}{dt}\right]_{chem} dt \tag{12}$$

### 4.2. The diffusion control function

The results of the isothermal simulation as described earlier always reach a final conversion of unity. These curves describe the chemically controlled kinetics. For the curing temperature of 100 °C, the conversion curves of the chemically controlled reaction $\alpha_{chem}(t)$ and the curve $\alpha(t)$ according to Eq. (11) are plotted together in Fig. 9.

As the chemically controlled kinetics $[d\alpha/dt]_{chem}$ is determined from the model-free kinetics, the diffusion control function is calculated by Eq. (5). The resulting curve is shown in the inset of Fig. 9.

The diffusion control function $f_d(\alpha)$ can be described with different model functions. The fit result

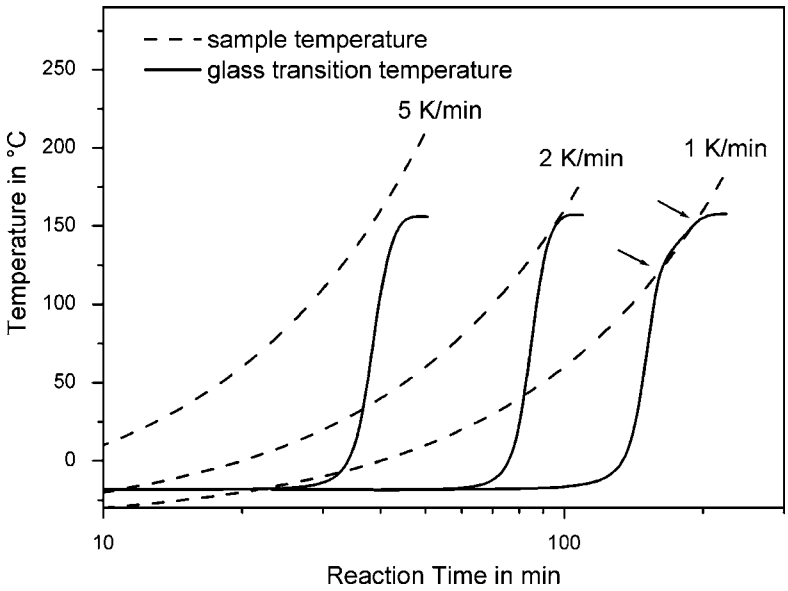


Fig. 8. Sample temperature (dashed line) and glass transition temperature (solid line) as a function of the reaction time for ramp curing experiments with different heating rates. For the calculation of the glass transition temperature curves Eq. (10) is used. The conversion bases on the curves in Fig. 1. The arrows at the curves for 1 K/min indicate vitrification and devitrification, respectively.

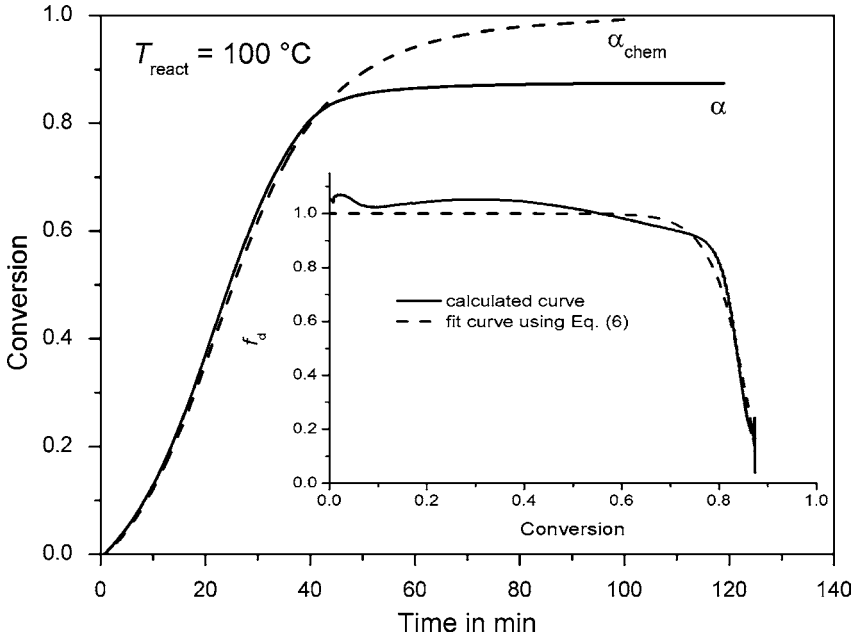


Fig. 9. Conversion as a function of the reaction time for an isothermal curing experiment at 100 °C. The experimental curve is shown by $\alpha$ and the conversion curve for a fictive experiment without diffusion control is represented by $\alpha_{chem}$ (calculated from the model-free kinetic results in Fig. 7). In the inset, the diffusion control function (solid line) is obtained by the quotient of the time derivatives of $\alpha(t)$ and $\alpha_{chem}(t)$. The dotted line is the best fit result using Eq. (6).

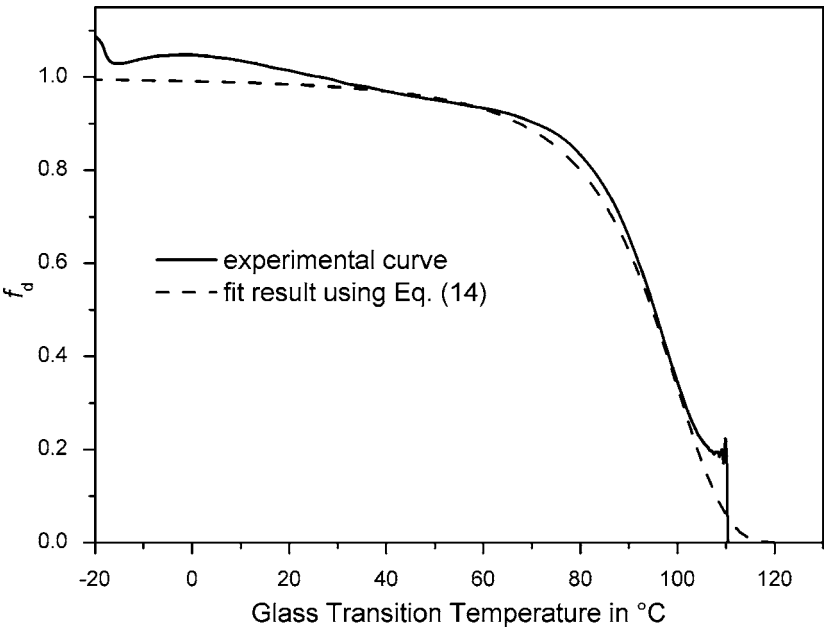


Fig. 10. The diffusion function of Fig. 9 vs. the glass transition temperature (solid line). The dashed line represents the curve calculated by the new model function (Eq. (14)). The parameter $\Delta T$ was selected to be 20 K. The reaction temperature is 100 °C.

of Eq. (6) with the parameters $\alpha_f = 0.88$ and $b = 0.044$ shows reasonable agreement (dashed curve in inset of Fig. 9). However, for the prediction of isothermal experiments Eq. (6) cannot be used in a reasonable way because both fit parameters depend on temperature [10].

In order to predict isothermal curing curves, we will introduce a new model function for $f_d(\alpha)$ which contains no temperature-dependent parameters. Because of the interaction between glass transition temperature, vitrification and diffusion-controlled reaction kinetics we express $f_d$ as a function of the glass transition temperature. The related curve is shown in Fig. 10. For the calculation of the conversion dependence of $T_g$, we use Eq. (10) in this work. The parameters are $D = 2.178$, $C_2 = 29.35$ K, $x_0 = 1.032$ and $T_{g1} = 189.1$ °C. For practical calculation, different equations for $T_g(\alpha)$ can also be used without major deviations.

As expected, the experimental diffusion control function shows an inflection point if the glass transition temperature is equal to the reaction temperature. A model function for $f_d(T_g(\alpha))$ has to describe this inflection point properly. Other predictions are the values at the limits: $f_d(T_g(\alpha = 0)) = 1$ and $f_d(T_g(\alpha_f)) = 1$. An equation fulfilling these conditions is

$$f_d(\alpha) = 1 - \left(1 + \left(\frac{T_0 - T_g(\alpha)}{A}\right)^3\right)^{-1} \tag{13}$$

where, $T_0$ and $A$ are constants. $T_0$ is the temperature at which the diffusion control function is zero. If we consider that this occurs at a temperature which is $\Delta T$ higher than the reaction temperature $T_{react}$, $T_0$ can be substituted with $T_{react} + \Delta T$. The inflection point condition delivers the expression for the constant $A = \sqrt[3]{2}\Delta T$. Finally, the new model function can be reduced to a one parametric function:

$$1f_d(\alpha, T_{react}) = 1 - \left(1 + \frac{1}{2}\left(\frac{T_{react} + \Delta T - T_g(\alpha)}{\Delta T}\right)^3\right)^{-1} \tag{14}$$

We assume that $\Delta T$ is related to the width of the glass transition, which is determined by a DSC cooling experiment of the fully cured material. This delivers the approximation $\Delta T = 20$ K. The resulting curve is

the dashed curve in Fig. 10. A comparison with the experimental curve shows good agreement between both curves.

### 4.3. Comparison of the kinetic predictions with experimental data

Using the chemically controlled function $\alpha_{chem}(t, T_{react})$ derived from model-free kinetics the vitrification time $t_v$ can be estimated using a model function (e.g. Eqs. (9) or (10)). First of all, the conversion $\alpha_v$ at which $T_g = T_{react}$ has to be calculated. In the second step, the related reaction time for $\alpha_v(t)$ are given from the model-free kinetics evaluation. This predicted vitrification time is calculated without any influence of diffusion control. A comparison with experimental data from [23] is shown in the time–temperature transition (TTT)-diagram in Fig. 11. At temperatures lower than 110 °C, the chemically controlled reaction yields a very good prediction of the vitrification time. For higher reaction temperatures, these calculated values of $t_v$ are significantly shorter than the measured ones.

To get better agreement with the measured data, diffusion control is considered. To do this, we will describe the kinetics during isothermal cure using Eq. (5). The chemically controlled kinetics are calculated from the model-free kinetic results in. Fig. 7. The parameter of the function $f_d$ in Eq. (14) was set to be $\Delta T = 20$ K. The only additional information that is needed is the relationship between $T_g$ and $\alpha$ (Fig. 3). With this information the isothermal curing curves can be simulated. From Eq. (5) follows the conversion:

$$\alpha(t) = \int_0^t \left[\frac{d\alpha}{dt}\right]_{chem} f_d(T_g(\alpha))\, dt \tag{15}$$

For the numerical solution of this integral equation, we use:

$$\Delta\alpha_i = (\alpha_{chem,i} - \alpha_{chem,i-1}) f_d(\alpha_{i-1} + \Delta\alpha_i) \tag{16a}$$

with

$$\alpha_i = \sum_{j=1}^{i} \Delta\alpha_j \tag{16b}$$

and start condition $\Delta\alpha_1 = \alpha_1 = \alpha_{chem,1}$. The indices $i$ and $j$ ($i, j = 1, 2, 3, \ldots$) describe the sampling points. Eq. (16) can be easily solved using standard mathematical software.

Selected conversion curves with and without consideration of diffusion control are shown in Fig. 12. For lower conversion, both simulated curves are identical. After a certain conversion (approximately 0.6 at 60 °C to 0.9 at 160 °C) the diffusion control leads to a deviation. The simulation considering diffusion control reaches a quasi constant final conversion which is

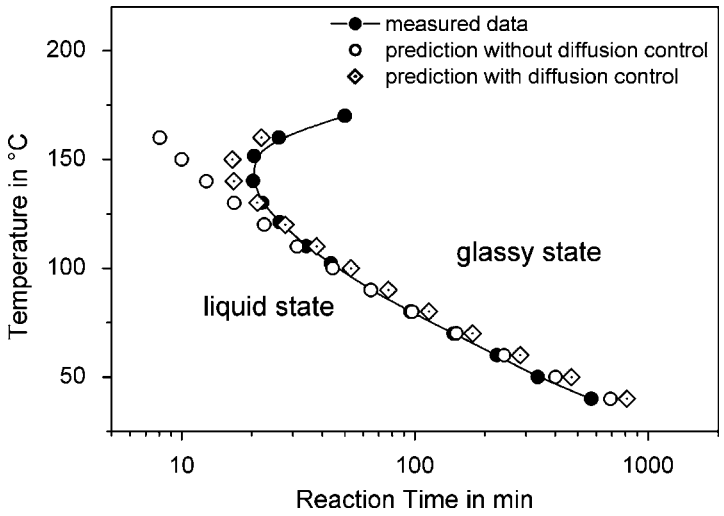


Fig. 11. TTT-diagram (vitrification time vs. the reaction temperature) for the isothermal cure of the system DGEBA–DDM. The filled circles represent measured results taken from [23], the open circles are calculated from the model-fee kinetics (Fig. 7), the diamonds are results of the simulation considering the diffusion control using Eqs. (5) and (14).

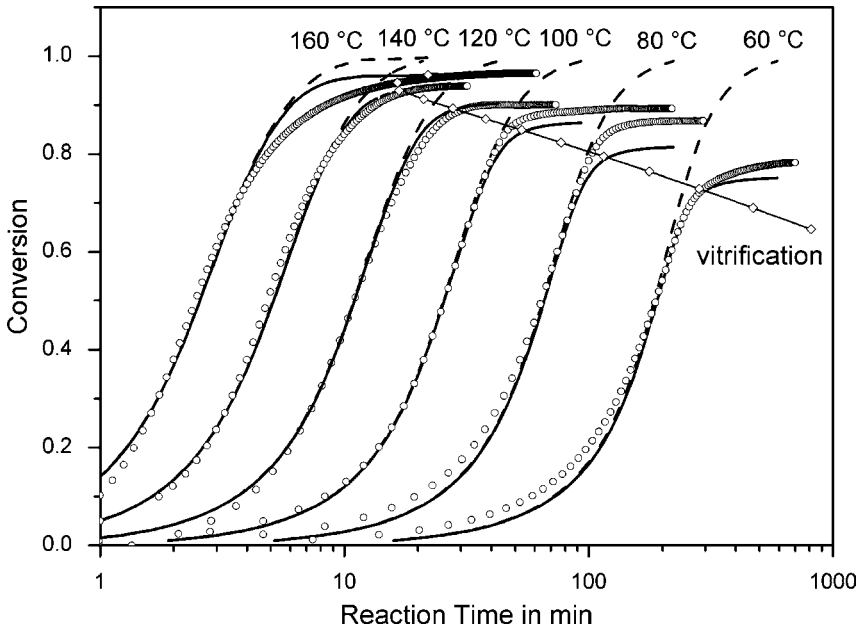


Fig. 12. Conversion as a function of the reaction time for the isothermal cure at different reaction temperatures. The dashed lines are the results of the fictive chemically controlled reaction calculated using model-free kinetics. The solid lines are simulated curves based on the dashed curves but considering the diffusion control function (Eq. (14)). The line with the diamonds characterizes the vitrification time determined from the simulated curves. For comparison, measured curves (from Fig. 2) are shown by the open circles.

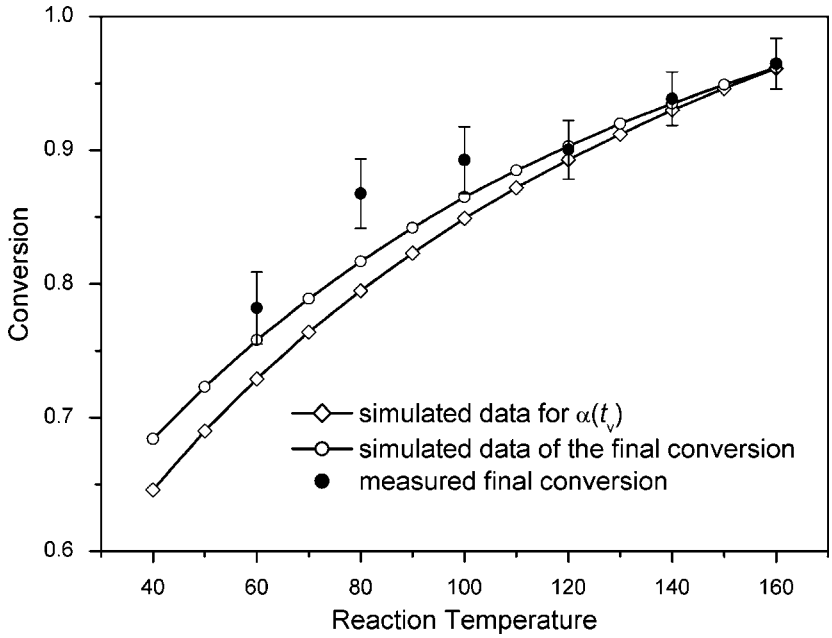


Fig. 13. The conversion at vitrification time (diamonds) and the final conversion (open circles) as a function of the isothermal reaction temperature calculated from the simulated curves (solid lines in Fig. 12). The filled symbols are measured values of the final conversion.

lower than unity. This final conversion increases with increasing temperature.

From the simulated conversion curves, $\alpha(t, T_{react})$ the vitrification time is calculated by $T_g(\alpha(t_v, T_{react})) = T_{react}$. The related vitrification curve is represented by the diamond line in Fig. 12. This data is also taken into the TTT-diagram ( diamonds in Fig. 11). It is shown that this new model of the diffusion control describes the vitrification time–temperature behavior consistently with experimental findings. In contrast to the vitrification time derived from $\alpha_{chem}$ the incorporation of the supposed function of $f_d(\alpha)$ into the model delivers the expected behavior, also for relatively high temperatures.

For comparison of the simulated curves with the measured curves from Fig. 2, the measured curves are also plotted in Fig. 12 (open circles). Small deviations occur towards the final conversion. The final conversion and the conversion at vitrification time as a function of the reaction temperatures are shown in Fig. 13. From the model, both the conversion at vitrification time $\alpha(t_v)$ and the final conversion $\alpha_f$ can be calculated. The distance between $\alpha(t_v)$ and $\alpha_f$ decreases with increasing temperature. Considering the experimental errors, the prediction of the final conversion is very good.

## 5. Conclusion

Using the isoconversional approach for the description of kinetic processes (model-free kinetics) the chemically controlled kinetics for curing processes of thermosetting systems can be evaluated from ramp curing measurements at sufficiently high heating rates. For this procedure, the material must not show vitrification. In order to ascertain this condition, we evaluate the relationship between the glass transition temperature $T_g$ and the conversion $\alpha$ during reaction. The function $T_g(\alpha)$ is measured by several post-curing experiments. To obtain an analytical expression a model function is taken as a fit function.

The chemically controlled kinetic function derived from model-free kinetics is used to describe the isothermal curing reaction in a temperature range below the final glass transition temperature. In order to consider the influence of diffusion control on kinetics, a new phenomenological equation for the diffusion control function with only one temperature independent parameter is introduced. To minimize the number of parameters in a first approximation, we have set the parameter $\Delta T$ as the width of the glass transition measured in a cooling run. It is shown that the simulated results agree with the experimental data (such as vitrification time, $\alpha(t_v)$ and final conversion) in a large temperature and time range. This agreement could be improved by optimization of the parameter $\Delta T$.

The procedure described can be used for predictions of the reaction kinetics of systems which vitrify during reaction and become diffusion-controlled. In addition to the knowledge of chemically controlled kinetics (taken from the model-free kinetic evaluation) one also needs to know the conversion dependence of the glass transition temperature. As a result, complex kinetics can be predicted using a minimum number of experiments.

## Acknowledgements

The author would like to thank Georg Widmann (Mettler-Toledo GmbH, Schwerzenbach, Switzerland) for helpful discussions and Sergey Vyazovkin (University of Alabama at Birmingham, USA) for helpful comments and the inspiration to the appendix.

## Appendix A. Alternative diffusion control functions

According to Eqs. (2) and (5), the kinetics can be described by

$$\frac{d\alpha}{dt} = k(T)f(\alpha)f_d(\alpha,T) = \left[\frac{d\alpha}{dt}\right]_{chem} f_d(\alpha, T) \qquad (A.1)$$

where, $k$ is the rate constant of the chemically controlled reaction. The diffusion control function $f_d$ depends on temperature and conversion. For comparison, we discuss $f_d$ in the terms of different kinetic approaches.

In the case of diffusion controlled cure, the model of Fischbeck–Rabinowitsh is often used for description of the empirical overall rate constant $k_e$ [26–28]:

$$\frac{1}{k_e} = \frac{1}{k} + \frac{1}{k_d} \qquad (A.2)$$

where, $k_d$ is the temperature and conversion dependent rate constant for the diffusion process. In this approach, a simple kinetic equation is:

$$\frac{d\alpha}{dt} = k_e(T,\alpha)f(\alpha) \tag{A.3}$$

Introduction of Eq. (A.2) in (A.3) yields:

$$\frac{d\alpha}{dt} = \frac{k(T)k_d(T,\alpha)}{k(T)+k_d(T,\alpha)}f(\alpha) \tag{A.4}$$

Comparison of Eq. (A.4) with (A.1) delivers an expression for the diffusion control function:

$$f_d(T,\alpha) = \frac{k_d(T,\alpha)}{k(T)+k_d(T,\alpha)} \tag{A.5}$$

In the early stage of the reaction, $k_d \gg k$. Thus, the diffusion control function is unity. After vitrification we assume $k_d \leq k$. Consequently, the limit of $f_d$ is zero.

An other approach of the interpretation of $f_d$, is assuming of a temperature dependent conversion function $f_T(\alpha, T)$:

$$f_T(T,\alpha) = f(\alpha)f_d(T,\alpha) \tag{A.6}$$

Such functions are discussed by Vyazovkin and Sbirrazzuoli [29]. One example introduced by these authors is:

$$f_T(T,\alpha) = (\alpha_f(T)-\alpha)^n \tag{A.7}$$

where, $\alpha_f(T) < 1$ is the maximum conversion of an isothermal cure at temperatures below the maximum glass transition temperature $T_{g1} = T_g(\alpha = 1)$ and $n$ describes the reaction order. In this case, $f_d$ follows from Eq. (A.6)

$$f_d(T,\alpha) = \left(\frac{\alpha_f(T)-\alpha}{1-\alpha}\right)^n \tag{A.8}$$

For interpretation of $f_d$ a combination of both approaches (Eqs. (A.5) and (A.8)) is possible. The diffusion control function is then:

$$f_d(T,\alpha) = \frac{k_d(T,\alpha)}{k(T)+k_d(T,\alpha)}\left(\frac{\alpha_f(T)-\alpha}{1-\alpha}\right)^n \tag{A.9}$$

All methods for the interpretation of $f_d$ are row descriptions in special cases and are only discussed to demonstrate the meaning of the diffusion function in terms of conventional kinetic approaches. From the physical point of view, these models have advantages and disadvantages. They are connected to the limits of the conventional kinetic models. A detailed discussion of these points is in preparation.

## References


[1] M.E. Brown, D. Dollimore, A.K. Galway, Reaction in Solid State, Comprehensive Chemical Kinetics, Vol. 22, Elsevier, Amsterdam, 1980.
[2] M.E. Brown, Introduction to Thermal Analysis, Chapman & Hall, New York, 1988.
[3] M.R. Kamal, Polym. Eng. Sci. 14 (1974) 231.
[4] S. Montserrat, J. Malek, Thermochim. Acta 228 (1993) 47.
[5] L.E. Nielson, J. Macromol. Sci. Rev. Macromol. Chem. C3 (1969) 69.
[6] J.K. Gillham, Polym. Eng. Sci. 26 (1986) 1429.
[7] G. Wisanrakkit, J.K. Gillham, J. Coat. Technol. 62 (1990) 35.
[8] S. Montserrat, J. Appl. Polym. Sci. 42 (1992) 545.
[9] J. Fournier, G. Williams, C. Duch, G.A. Aldridge, Macromolecules 29 (1996) 7097.
[10] W. Jenninger, J.E.K. Schawe, I. Alig, Polymer 41 (2000) 1577.
[11] M.E. Brown, A.K. Galway, Thermochim. Acta 110 (1979) 129.
[12] T. Ozawa, Bull. Chem. Soc. Jpn. 38 (1965) 1881.
[13] J.H. Flynn, L.H. Wall, J. Res. Natl. Bur. Stand. Sect. A 70 (1966) 487.
[14] S. Vyazovkin, Thermochim. Acta 211 (1992) 181.
[15] S. Vyazovkin, W. Linert, Anal. Chim. Acta 295 (1994) 101.
[16] S. Vyazovkin, N. Sbirrazzuoli, Macromolecules 29 (1996) 1867.
[17] S. Vyazovkin, New J. Chem. 24 (2000) 913.
[18] E. Lerroy, J. Dupuy, A. Maazouz, Macromol. Chem. Phys. 202 (2001) 465.
[19] J.E.K. Schawe, J. Thermal Anal. Cal. 64 (2001) 599.
[20] J.P. Pascault, R.J.J. Williams, J. Polym. Sci., Part B. Polym. Phys. 28 (1990) 85.
[21] M.J. Richardson, Comprehensive Polymer Science, in: C. Booth, C. Price (Eds.), Vol. 1, Pergamon Press, Oxford, 1989, p. 867.
[22] S.L. Simon, J.K. Gillham, J. Appl. Polym. Sci. 47 (1993) 461.
[23] J.E.K. Schawe, Thermochim. Acta, accepted.
[24] S. Montserrat, J. Polym. Sci., Part B. Polym. Phys., submitted for publication.
[25] S. Vyazovkin, J. Thermal Anal. 49 (1997) 1493.
[26] E. Rabinowitch, Trans. Faraday Soc. 33 (1937) 1225.
[27] K. Fischbeck, Z. Electrochem. 39 (1933) 316.
[28] K. Fischbeck, L. Neundeubel, F. Salzer-Tübingen, Z. Electrochem. 40 (1934) 517.
[29] S. Vyazovkin, N. Sbirrazzuoli, Macromol. Rapid Commun. 21 (2000) 85.